

## CFD simulation of heat transfer in ferrofluids

A. Jafari,<sup>a</sup> T. Tynjälä,<sup>a</sup> S.M. Mousavi,<sup>b,c</sup> P. Sarkomaa<sup>a</sup>

<sup>a</sup> *Laboratory of Engineering Thermodynamics, Lappeenranta University of Technology, Lappeenranta, Finland*

<sup>b</sup> *Department of Chemical and Petroleum Engineering, Sharif University of Technology, Tehran, Iran*

<sup>c</sup> *Department of Chemical Engineering, Lappeenranta University of Technology, Lappeenranta, Finland*

### Abstract

In this work time dependent heat transfer flow through a kerosene based ferrofluid is considered. The flow is in a cylindrical geometry with the height and diameter of 10 mm. Computational fluid dynamics was used to simulate the system. In CFD simulations mixture model was applied to describe the behavior of the magnetic particles. A uniform magnetic field with different strengths and directions were used over the system. Numerical results illustrate that compare to the field free case, in the presence of magnetic field the transport processes will enhance. It was also shown that when magnetic field is perpendicular to the temperature gradient, the heat transfer will increase more compare to the case with magnetic field parallel to temperature gradient.

Keywords: CFD simulation, heat transfer, ferrofluid

### 1. Introduction

Ferrofluids are composed of magnetic nanoparticles and carrier fluid [1]. They are a type of functional fluids whose flow and energy transport processes can be controlled by adjusting an external magnetic field, which makes it find a variety of applications in various fields. Fore example using ferrofluids in miniaturized devices and external magnetic field enhance convection in these devices [2].

The relationship between an imposed magnetic field, the resulting ferrofluid flow and the temperature distribution is not understood well enough, and the references regarding heat transfer with magnetic fluids is relatively sparse [2]. In this work time dependent heat transfer through a ferrofluid in a cylinder under the influence of magnetic field strength was simulated.

### 2. Governing Equations

Here the magnetic fluid is considered electrically non-conductive, and Maxwell's equations can be written as follows:

$$\nabla \cdot \mathbf{B} = 0, \tag{1}$$

$$\nabla \times \mathbf{H} = 0, \quad (2)$$

where  $\mathbf{B}$  is the magnetic induction, and  $\mathbf{H}$  is the magnetic field vector. Further the magnetic induction, the magnetization vector,  $\mathbf{M}$ , and the magnetic field vector are related by the constitutive relation:

$$\mathbf{B} = \mu_0(\mathbf{M} + \mathbf{H}), \quad (3)$$

where  $\mu_0$  is a magnetic permeability in vacuum.

Magnetic scalar potential,  $\phi_m$ , is defined as

$$\mathbf{H} = -\nabla \phi_m. \quad (4)$$

Using Maxwell's equations, the flux function for magnetic scalar potential,  $\phi_m$ , may be written as

$$\nabla \cdot \left[ \left( 1 + \frac{\partial \mathbf{M}}{\partial \mathbf{H}} \nabla \phi_m \right) \right] = \nabla \cdot \left[ \left( \frac{\partial \mathbf{M}}{\partial T} (T - T_0) + \frac{\partial \mathbf{M}}{\partial \alpha_p} (\alpha_p - \alpha_{p_0}) \right) \right] \quad (5)$$

where  $\alpha_p$ ,  $T$  and subscript 0 represent the volume fraction of magnetic particles, temperature and initial conditions, respectively. Within the simulations  $\frac{\partial \mathbf{M}}{\partial \mathbf{H}} = \chi$ ,  $\frac{\partial \mathbf{M}}{\partial T} = -\beta_m \mathbf{M}_0$  and  $\frac{\partial \mathbf{M}}{\partial \alpha_p}$  are assumed constant and using Langevin equation they can be defined [3].

It is assumed that the magnetic fluid treats as a two phase mixture of magnetic particles in a carrier phase. This model allows interpenetration of phases and their moving at different velocities by using the concept of slip velocities. The continuity, momentum, and energy equations for the mixture and the volume fraction equation for the secondary phases, as well as algebraic expressions for the relative velocities are solved. The governing equations are as follow:

$$\frac{\partial}{\partial t} (\rho_m) + \nabla \cdot (\rho_m \bar{\mathbf{v}}_m) = 0 \quad (6)$$

$$\frac{\partial}{\partial t} (\rho_m \bar{\mathbf{v}}_m) + \nabla \cdot (\rho_m \bar{\mathbf{v}}_m \bar{\mathbf{v}}_m) = -\nabla P_m + \mu_m \nabla^2 \bar{\mathbf{v}}_m - \quad (7)$$

$$\nabla \cdot \left( \alpha_p \rho_p \bar{\mathbf{v}}_{Mp} \bar{\mathbf{v}}_{Mp} + \alpha_c \rho_c \bar{\mathbf{v}}_{Mc} \bar{\mathbf{v}}_{Mc} \right) + \rho_m g + \alpha_p \frac{m_p}{V_p} L(\xi) \nabla H$$

$$\frac{\partial}{\partial t} (\rho_m c_{v,m} T) + \nabla \cdot \left[ \left( \alpha_p \rho_p \bar{\mathbf{v}}_p c_{p,p} + \alpha_c \rho_c \bar{\mathbf{v}}_c c_{p,c} \right) T \right] = \nabla \cdot (k_m \nabla T) \quad (8)$$

where  $\rho$ ,  $\bar{\mathbf{v}}$ ,  $P$ ,  $\mu$ ,  $\xi$ , and  $k$  are density, velocity, pressure, dynamic viscosity, Langevin parameter and conductivity, respectively. The subscripts m, p and c refer to the mixture, magnetic particles and carrier fluid, respectively and  $\bar{\mathbf{v}}_{Mi} = \bar{\mathbf{v}}_i - \bar{\mathbf{v}}_m$  is diffusion velocity. From the continuity equation for secondary phase, the volume fraction equation for magnetic phase can be obtained:

$$\frac{\partial}{\partial t} (\alpha_p \rho_p) + \nabla \cdot \left( \alpha_p \rho_p (\bar{\mathbf{v}}_m - \bar{\mathbf{v}}_{dr,p}) \right) = 0 \quad (9)$$

where  $\vec{v}_{dr,p}$  is drift velocity. With considering to forces act on a single magnetic particle, the slip velocity is defined similar to [3]

$$\vec{v}_s = \vec{v}_p - \vec{v}_c = \frac{m_p L(\xi)}{3\pi\mu_c d_p} \nabla H + \frac{d_p^2 (\rho_p - \rho_c)}{18\pi\mu_c} g \quad (10)$$

where  $d_p$  is the magnetic particle diameter.

### 3. Numerical Method

In this research commercial software, Gambit, was used to create the geometry and generate the grid. To divide the geometry into discrete control volumes, about  $5.9 \times 10^5$  tetrahedral computational cells,  $1.2 \times 10^6$  triangular elements, and more than  $10^5$  nodes were used. The results are grid independent. A grid independency check has been performed at temperature difference of 100 K over the cylinder and magnetic field strength 160 kA/m parallel to the temperature gradient. Concentration difference of dispersed phase or separation after 100 s was considered to compare grids, and results have been shown in table 1. As the difference between numerical results in grids 2 and 3 is less than 6%, so to save cost and time grid 2 has been chosen for all tests.

Grid	1	2	3
Numerical results (percent of concentration difference)	6.5	9.5	9
Number of tetrahedral elements	$10^5$	$5.9 \times 10^5$	$1.3 \times 10^6$
Number of nodes	$1.9 \times 10^4$	$10^5$	$2.3 \times 10^5$

Table 1: Percentage of phase separation at different grids

Numerical simulations were done by commercial software, Fluent, and a user defined function was added to apply a uniform external magnetic field parallel to the temperature gradient. All equations were solved using second order upwind scheme. Constant temperature boundary conditions were applied for both bottom and top of the cylinder, and uniform external magnetic field was subjected parallel to the temperature gradient.

### 4. Results and Discussion

Fig. 1(a) depicts a schematic diagram used in the present simulations and the grid is illustrated in Fig. 1(b). A kerosene-based magnetic fluid with magnetization 48 kA/m, particle diameter 9 nm, and solid volume fraction 2% was used in this study.

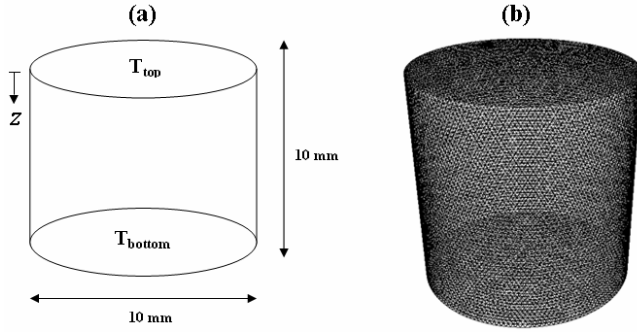


Fig. 1: (a) Schematic of the geometry, (b) The grid used in this study

Other properties of the studied fluid are shown in table 2. It is assumed that the Density of carrier liquid, kerosene, changes with average temperature according to the following equation

$$\rho_c = 1248 - 1.56 \times T. \quad (11)$$

Properties of the mixture except viscosity can be calculated as follow

$$N_m = \sum_{i=1}^{i=2} \alpha_i N_i \quad (12)$$

where  $N$  represents any property, and  $i$  refers to both continuous and dispersed phase. Dynamic viscosity of mixture can be shown as [4]

$$\mu_m = \left( 1 + \frac{5}{2} \alpha_{p0} \right) \mu_c. \quad (13)$$

Property	Value	Property	Value
Density ( $p$ )	$5400 \text{ kg/m}^3$	Heat capacity at constant pressure ( $c$ )	$2090 \text{ J/kgK}$
Thermal conductivity ( $c$ )	$0.149 \text{ W/mK}$	Heat capacity at constant pressure ( $p$ )	$4000 \text{ J/kgK}$
Thermal conductivity ( $p$ )	$1 \text{ W/mK}$	Particle magnetic moment	$2.5 \times 10^{-19} \text{ Am}^2$
Dynamic viscosity ( $c$ )	$0.0024 \text{ kg/ms}$	Vacuum permeability	$4\pi \times 10^{-7} \text{ H/m}$
Dynamic viscosity ( $p$ )	$0.03 \text{ kg/ms}$	Thermal expansion coefficient	$0.008 \text{ 1/K}$

Table 2: Properties of the studied ferrofluid. Here  $c$  and  $p$  illustrate continuous and dispersed phase, respectively.

The temperature difference 10 K was applied to the cylinder. The heat transfer characteristic of the ferrofluid in the presence and absence of a uniform magnetic field is given in Fig. 2. As can be expected heat flux is enhanced under an applied magnetic

field. This fact confirmed experimentally by Jeyadevan et al. [5]. To investigate the effect of natural convection, a set of simulations at the same conditions, but in the absence of any convection was done. Comparison of obtained results showed that in the presence of natural convection heat transfer will increase. Since the temperature gradient in the cylinder was not very high, the difference between two conditions, with and without natural convection, was not significant.

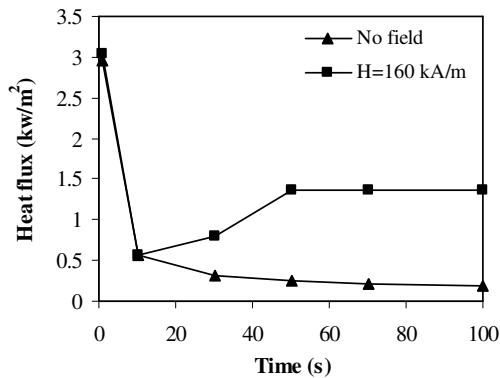


Fig. 2: Effect of magnetic field on heat flux in the presence of natural convection

To test the effect of natural convection more simulations were performed at temperature difference of 40 K and different magnetic fields. Results at H=160 kA/m are presented in Fig. 3, and it is clear that with increase of temperature gradient the effect of natural convection will improve. In addition it is found that effect of temperature gradient on heat transfer of ferrofluids is more than magnetic field.

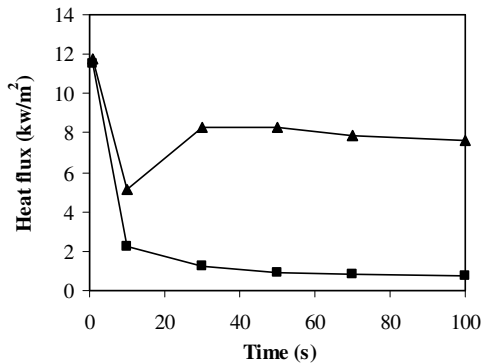


Fig. 3: Heat transfer in the ferrofluid versus time. Triangles and squares show the conditions with and without natural convection, respectively.

Figure 4 illustrates fluid streamlines color coded using velocity magnitude. These kinds of vortices observed in the presence of natural convection play an important role in transport mechanism of flow, and increase heat transfer in the system. In the absence of natural convection, this kind of vortices has been observed locally, which means that rolls are close to the domain boundaries.

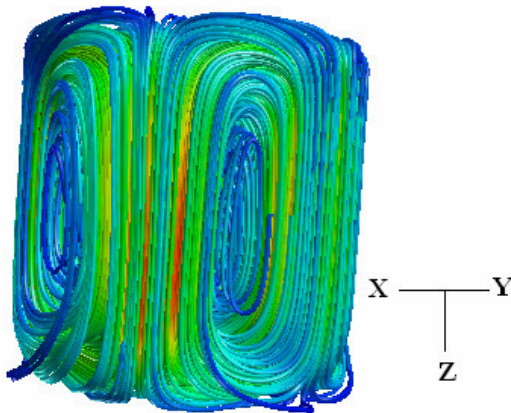


Fig. 4: Fluid streamlines at  $H=160$  kA/m and temperature difference 10 K

Number of Rayleigh rolls depends on different parameters such as temperature difference and aspect ratio. Any variation of these quantities can induce a change in behaviour of the fluid. At aspect ratio 1, magnetic field 160 kA/m, and temperature difference 10 K four rolls have been observed. As Fig. 5 illustrates with passing time the system becomes more stable and symmetric.

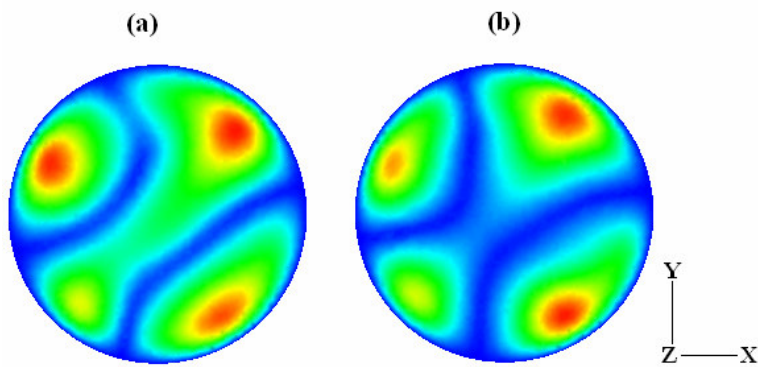


Fig. 5: Rayleigh rolls on a plane at  $z=0.005$  m after (a) 50 s and (b) 100 s

To test the effect of magnetic field direction, a uniform magnetic field in parallel and perpendicular to the temperature gradient direction has been applied. The velocity profiles showed that for the second condition the velocity is higher than the situation with parallel direction to the temperature gradient. According to the results the heat transfer increases for perpendicular orientation of magnetic field and temperature gradient directions.

## 5. Conclusion

In this work CFD simulations were carried out in order to study the effect of external magnetic field on heat transfer in ferrofluids. It was found that the transferred heat is a function of magnetic field strength and its direction. Results showed that heat transfer can be increased by applying magnetic field perpendicular to the temperature

gradient. The heat transfer efficiency can be further improved by optimizing the magnetic field strength, direction, and distribution.

### **Acknowledgements**

Authors would like to acknowledge the Academy of Finland Grant No. 110852 for the support of this work.

### **References**

- [1] Xuan, Y., Ye, M. and Li, Q., (2005) *International Journal of Heat and Mass Transfer*, 48, 2443–2451.
- [2] Streck, T. and Jopek, H., (2007), *Phys. Stat. Sol. (b)*, 1–11(DOI 10.1002/pssb.200572720).
- [3] Bozhko, A. and Tynjälä, T., (2005) *Journal of Magnetism and Magnetic Materials*, 289,281–284.
- [4] Rosensweig, RE., *Ferrohydrodynamics*, 2<sup>nd</sup> ed., Dover Publications Inc., New York (1997).
- [5] Jeyadevan, B., Koganezawa, H. and Nakatsuka, K., (2005) *Journal of Magnetism and Magnetic Materials*, 289,253–256.